

See discussions, stats, and author profiles for this publication at: <https://www.researchgate.net/publication/275256083>

Design of (X-DADAD) n Type Copolymers for Efficient Bulk Heterojunction Organic Solar Cells

ARTICLE *in* MACROMOLECULES · APRIL 2015

Impact Factor: 5.8 · DOI: 10.1021/ma5023956

CITATIONS

2

READS

63

8 AUTHORS, INCLUDING:



Oleg V. Kozlov

University of Groningen

5 PUBLICATIONS 7 CITATIONS

[SEE PROFILE](#)



A. V. Chernyak

Russian Academy of Sciences

45 PUBLICATIONS 87 CITATIONS

[SEE PROFILE](#)



Pavel A Troshin

Russian Academy of Sciences

180 PUBLICATIONS 2,124 CITATIONS

[SEE PROFILE](#)

Design of (X-DADAD)_n Type Copolymers for Efficient Bulk Heterojunction Organic Solar Cells

Alexander V. Akkuratov,[†] Diana K. Susarova,[†] Oleg V. Kozlov,^{‡,||} Alexander V. Chernyak,[†] Yuryi L. Moskvin,[§] Lubov A. Frolova,[†] Maxim S. Pshenichnikov,[‡] and Pavel A. Troshin*,[†]

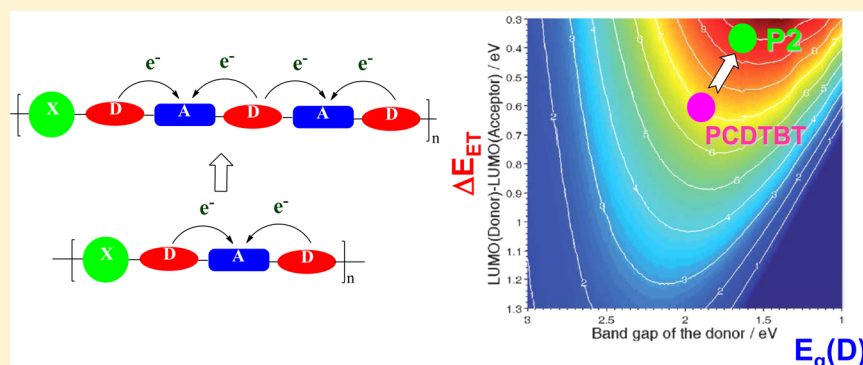
[†]Institute for Problems of Chemical Physics, Russian Academy of Sciences, Semenov Prospect 1, Chernogolovka 142432, Russian Federation

[‡]Zernike Institute of Advanced Materials, University of Groningen, Nijenborgh 4, 9747 AG Groningen, The Netherlands

[§]Institute for Energy Problems of Chemical Physics, Russian Academy of Sciences (Branch), Semenov Prospect 1/10, Chernogolovka, Moscow Region 142432, Russian Federation

^{||}Faculty of Physics & International Laser Center, Lomonosov Moscow State University, Leninskie Gory 1, 119991, Moscow, Russia

Supporting Information



ABSTRACT: We show that extended TBTBT structure (T = thiophene, B = benzothiadiazole) can be used as an electron-deficient building block for designing conjugated polymers with deeply lying HOMO energy levels and narrow band gaps. The first carbazole–TBTBT copolymer **P2** demonstrated power conversion efficiencies exceeding 6% in bulk heterojunction solar cells in combination with advanced operational stability, unlike conventional donor polymers such as PTB7, PBDTTT-CF, etc.

INTRODUCTION

The efficiency of organic fullerene/polymer bulk heterojunction solar cells has been increased dramatically during the past few years mainly due to design and implementation of novel electron donor materials with advanced optoelectronic properties.¹ The vast majority of promising conjugated polymers were built using so-called “push–pull” architecture by combining different electron-deficient heterocycles such as quinoxaline,² benzothiadiazole,³ 1,4-diketopyrrolopyrrole,⁴ thieno[3,4-*b*]-thiophene,⁵ thieno[3,4-*c*]pyrrole-4,6-dione,⁶ and isoindigo⁷ with electron-rich thiophene units or thiophene-based heterocycles such as cyclopentadithiophene,⁸ dithienobenzene,⁹ or dithienosilole¹⁰ in alternating copolymer structure. The recent progress in the field is reviewed in a number of publications.¹¹ As long as the efficiency of organic solar cells was substantially improved, there appeared major concerns regarding their stability.¹²

Among hundreds of investigated polymers, the carbazole-TBT copolymer PCDTBT¹³ has demonstrated an outstanding stability. In particular, the lifetime of PCBM/PCDTBT solar cells was estimated to be in the range of at least 6–8 years,

which is substantially longer as compared to the P3HT/PCBM-based devices.¹⁴ Nonetheless, optoelectronic properties of PCDTBT are not optimized with respect to PCBM used as electron acceptor counterpart because of a 0.55 eV LUMO–LUMO offset (Figure 1a). As a consequence, efficiency of organic solar cells based on this material combination can

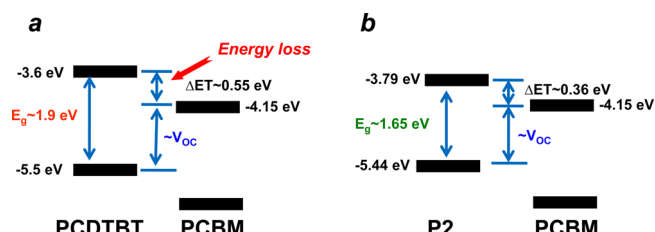


Figure 1. Frontier energy levels of PCDTBT/PCBM (a) and P2/PCBM (b) binary systems.

Received: November 26, 2014

Revised: March 9, 2015

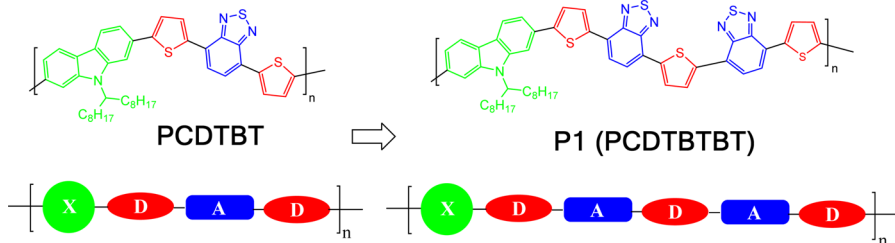


Figure 2. Schematic illustration of the approach to design of novel conjugated polymers pursued in this work.

hardly exceed 7%.¹⁵ The reported reproducible experimental solar cell efficiencies for PCDTBT/[70]PCBM blends fall in the range of 5.6–6.6%.¹⁶ The energy diagram for the PCDTBT–PCBM system (Figure 1) suggests that optoelectronic properties of the polymer can be improved by lowering its LUMO energy without affecting significantly the HOMO position.

A number of previous attempts to modify the chemical structure of PCDTBT in order to lower its LUMO energy and/or reduce its band gap were unsuccessful and resulted in inferior solar cell performances (see examples in Figure S1 and Table S1, Supporting Information).

The approach pursued in this work is outlined schematically in Figure 2.

The PCDTBT repeating unit comprises in its molecular framework the electron-deficient benzothiadiazole unit (acceptor “A”), two adjacent electron donor thiophene rings (donor “D”), and carbazole unit “X” which is a considerably weaker electron donor compared to the thiophene.¹⁷ Therefore, PCDTBT represents an example of the $(-\text{X}-\text{DAD})_n$ family of conjugated polymers. We proposed to introduce additional alternating A and D elements in the polymer repeating unit thus opening a pathway toward $(-\text{X}-\text{DADAD})_n$ copolymers which are expected to have advanced optoelectronic properties compared to conventional $(-\text{X}-\text{DAD})_n$ structures, particularly, lower LUMO energies and narrower band gaps.

It should be noted that alternated donor–acceptor systems are extensively utilized in the design of small molecular electron donor materials for organic solar cells. A number of high efficiency DADAD, DADADAD, and even DADADADAD systems have been explored recently.¹⁸ Surprisingly, a potential of this highly promising approach was not utilized in the development of electron donor polymers for bulk heterojunction solar cells. In the present work we report the application of this concept for designing a novel carbazole–thiophene–benzothiadiazole copolymer, demonstrating high photovoltaic performance in combination with an improved stability.

EXPERIMENTAL SECTION

General. All solvents and reagents were purchased from Sigma-Aldrich or Acros Organics and used as received or purified according to standard procedures. [70]PCBM and PCDTBT ($M_w \sim 200\,000$ g/mol, PDI = 5–6) were synthesized and purified using previously reported procedures.^{19,15} PTB-7, PBDTTT-CF, and PDTSTPD were products of 1-Material Inc. (Quebec, Canada). Poly(3-hexylthiophene) of EE grade was purchased from Rieke Metals Co. AFM images were obtained using NTEGRA PRIMA instrument (NT-MDT, Russia).

Molecular weight characteristics of conjugated polymers were obtained using Shimadzu LC20 instrument equipped with a Phenomenex Luna Phenogel 5 μm column (0.78×30 cm, 5–500 kDa). The measurements were performed using freshly distilled THF

or toluene as eluents (flow rate 0.5 mL/min). The column was calibrated using a series of commercial polystyrene standards obtained from Fluka (THF as eluent) or using custom-made F8BT standards with PDI < 1.5 (toluene used as eluent).

Synthesis of 1. Compound 1 was prepared from 4,7-dibromo-2,1,3-benzothiadiazole (1.0 g, 3.40 mmol), 2-(tributylstanny)-thiophene (1.28 g, 3.43 mmol), and tetrakis(triphenylphosphine)-palladium(0) (0.026 g, 0.022 mmol) using a procedure reported previously.²⁰

Synthesis of 2 and 3. Compound 2 was synthesized using 1 (2.97 g, 10 mmol), 2,5-bis(tributylstanny)thiophene (3.31 g, 5 mmol), and Pd(PPh₃)₄ (0.023 g, 0.02 mmol). Compound 3 was obtained by bromination of 2 with NBS (N-bromosuccinimide) in warm 1,2-dichlorobenzene (55 °C for 60 h). Detailed procedures and spectral characteristics were reported previously.²¹

Synthesis of 5. Compound 3 (1.0 g, 1.5 mmol) and (3-(2-ethylhexyl)thiophen-2-yl)boronic acid (1.2 g, 5.0 mmol) were placed under argon in a two-necked flask equipped with a reflux condenser. Afterward, toluene (50 mL), 2 M aqueous solution of K₂CO₃ (2 mL), Aliquat 336 (1 drop, ca. 80 mg), and tetrakis(triphenylphosphine)-palladium(0) (10 mg) were added in the listed here sequence. The obtained reaction mixture was stirred vigorously at 90–100 °C. The course of the reaction was monitored with HPLC. The synthesis was terminated when starting compound 3 disappeared and the amount of monofunctionalization product was below 5%. The mixture was poured into water and extracted with chloroform. Organic layer was then dried over anhydrous MgSO₄. Finally, the solvent was removed at the rotary evaporator, producing a viscous oily residue. The crude product was dissolved in 40 mL of toluene and filtered through a syringe filter (PTFE, 0.45 μm). The solution was processed further using a preparative Shodex GPC column (20 mm × 300 mm) and toluene as eluent which resulted in isolation of pure precursor compound. The latter was brominated using stoichiometric amount of NBS in 1,2-dichlorobenzene at RT to afford the title compound 5 in 60–67% overall yield.

5: ¹H NMR (CDCl₃, 600 MHz): δ (ppm) 8.07 (s, 2H), 7.96 (d, J = 3.8 Hz, 2H), 7.81 (d, J = 7.7 Hz, 2H), 7.72 (d, J = 7.7 Hz, 2H), 7.06 (d, J = 3.8 Hz, 2H), 6.85 (s, 2H); 2.68 (d, J = 7.2 Hz, 4H), 1.63 (m, 2H), 1.25–1.34 (m, 16H), 0.85 (m, 12H). ¹³C NMR (CDCl₃, 126 MHz): δ (ppm) 152.44, 152.39, 140.47, 139.91, 139.35, 133.33, 132.65, 130.35, 128.44, 127.87, 127.73, 127.21, 125.52, 125.42, 125.11, 110.76, 40.34, 33.64, 32.69, 28.80, 25.84, 23.13, 14.18, 10.84.

Synthesis of P1. Monomers 3 (195 mg, 0.297 mmol) and 4 (200 mg, 0.297 mmol) were introduced into a 50 mL round-bottom three-necked flask equipped with a thermometer and a reflux condenser. Toluene (35 mL), 2 M aqueous solution of K₂CO₃ (0.6 mL), Aliquat 336 (1 drop, ca. 80 mg), and tetrakis(triphenylphosphine)-palladium(0) (10 mg) were added in the listed here sequence. The reaction mixture was degassed, immersed into an oil bath, and heated at reflux. The molecular weight characteristics of the formed product were controlled every 30 min. The reaction was stopped when the polymer started to precipitate from the reaction mixture. The 4,4,5,5-tetramethyl-2-phenyl-1,3,2-dioxaborolane (4.0 mg, 0.019 mmol) was added, and the reaction mixture was heated for an additional 25 min. Afterward, an excess of bromobenzene (300 mg, 1.9 mmol) was introduced, and the mixture was stirred at reflux for another 25 min. Then the mixture was cooled down to room temperature, and 50 mL

of toluene was added. The resulting organic layer containing finely dispersed precipitate of **P1** was washed three times with deionized water (50 mL) and poured to 60 mL of 2-propanol. The precipitated polymer flakes were filtered into the cellulose thimble and processed using Soxhlet extraction with hexanes (12 h), acetone (12 h), dichloromethane (12 h), chloroform (8 h), chlorobenzene (12 h), and 1,2-dichlorobenzene (12 h). A considerable part of the polymer remained undissolved in the thimble. The 1,2-dichlorobenzene extract was concentrated in vacuum to 45 mL and poured in methanol (90 mL). The obtained solid was collected by filtration and dried under vacuum. The polymer **P1** was obtained as dark green, almost black, flakes with a yield of 106 mg (40%). $M_w = 29\,100$ g/mol, $M_w/M_n = 3.3$. UV-vis: $\lambda_{max} = 369, 407$, and 582 nm; $\lambda_{edge} = 726$ nm.

Synthesis of P2. Monomers **4** (657.6 mg, 1.0 mmol) and **5** (1063 mg, 1.0 mmol) were introduced into a 50 mL round-bottom three-necked flask equipped with a thermometer and a reflux condenser. Toluene (25 mL), 2 M aqueous solution of K_2CO_3 (2 mL), Aliquat 336 (1 drop, ca. 80 mg), and tetrakis(triphenylphosphine)-palladium(0) (10 mg) were added in the listed here sequence. The reaction mixture was degassed, immersed into an oil bath, and heated at reflux for 3–6 h. The molecular weight characteristics of the formed product were controlled every 30 min. The reaction was intentionally terminated when the weight-average molecular weight M_w reached ca. 150 000 g/mol. The 4,4,5,5-tetramethyl-2-phenyl-1,3,2-dioxaborolane (4.0 mg, 0.019 mmol) was added, and the reaction mixture was heated for additional 25 min. Afterward, an excess of bromobenzene (300 mg, 1.9 mmol) was introduced, and the mixture was stirred at reflux for another 25 min. Then the mixture was cooled down to room temperature, and the polymer was extracted with 500 mL of toluene; the resulting solution was washed three times with deionized water (250 mL), dried, and concentrated under vacuum (rotary evaporator) to 40 mL. Addition of 150 mL of methanol precipitated the crude polymer. Subsequent purification was achieved using several additional dissolving/precipitation cycles. Finally, the precipitated polymer flakes were filtered into the cellulose thimble and processed using Soxhlet extraction with hexanes (12 h), acetone (12 h), dichloromethane (12 h), chloroform (8 h), and chlorobenzene (12 h). A very minor amount of the polymer remained undissolved as a residue in the thimble. The chlorobenzene extract was concentrated under vacuum to the volume of ca. 20 mL, diluted with 20 mL of 1,2-dichlorobenzene, and precipitated in methanol. The obtained dark green (almost black) solid was collected by filtration and dried under vacuum. The total yield of the purified polymer **P2** varied between 70 and 85% depending on the applied number of dissolving/precipitation cycles.

Cyclic Voltammetry Measurements. The cyclic voltammetry measurements were performed for thin films (150–250 nm thick) of polymers **P1**, **P2**, and PCDTBT deposited on a glassy carbon disc electrode (working electrode, $d = 5$ mm, BAS Inc.) by drop-casting from a 1-chloronaphthalene–1,2-dichlorobenzene (1:1 v/v) mixture in the case of **P1** and a chlorobenzene–chloroform (1:4 v/v) mixture in the case of **P2**. The measurements were performed in a three-electrode electrochemical cell using 0.1 M solution of Bu_4NPF_6 in acetonitrile as supporting electrolyte, platinum wire as a counter electrode, and a silver wire immersed in 0.01 M solution of $AgNO_3$ in 0.1 M TBAP (CH_3CN) as a reference Ag/Ag^+ electrode (BAS Inc.). Ferrocene was used as internal reference. The electrolyte solution was purged with argon before the measurements. The voltammograms were recorded using an ELINS P-30SM instrument at room temperature with a potential sweep rate of 50 mV/s.

Fabrication and Characterization of Photovoltaic Devices. The conjugated polymer **P2** (7 mg) and [70]PCBM (14 mg) were dissolved together in 1 mL of 1,2-dichlorobenzene while stirring at room temperature for 48 h. 1,8-Diodooctane (DIO) was added to the blend solution to achieve 0.63% volume concentration. The prepared solution was filtered through the PTFE 0.45 μ m syringe filter and subjected to spin-coating at 900–1100 rpm for 150 s on the top of the annealed PEDOT:PSS (Clevios HTL) films deposited on the patterned ITO electrodes (see ref 22 for a general description of the substrate preparation procedure). The obtained films were transferred immediately inside glovebox and thermally annealed in an argon

atmosphere at 90 °C for 10 min. The top electrode comprising Ca (20 nm) and Ag (100 nm) was deposited by thermal evaporation at the pressure below 4×10^{-6} mbar in a vacuum chamber integrated inside a MBraun glovebox.

The current–voltage (I – V) characteristics of the devices were obtained in dark and under the simulated 100 mW/cm² AM1.5 solar irradiation provided by a KHS Steuernagel solar simulator integrated in MBraun glovebox. The intensity of the illumination was checked every time before the measurements using a calibrated silicon diode with a known spectral response. The I – V curves were recorded in inert atmosphere using Keithley 2400 source-measurement unit. The external quantum efficiency spectra (EQE) were measured in normal air atmosphere without applying any special encapsulation or protection to the photovoltaic devices using a specially designed setup (LOMO instruments, Russia).

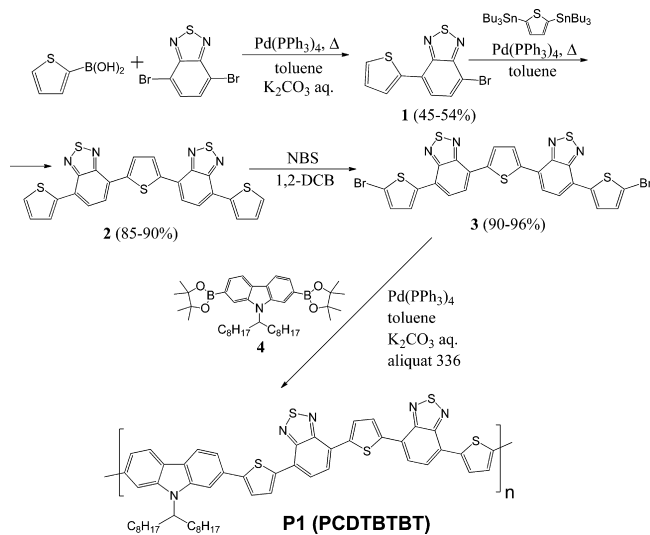
Ultrafast PIA Spectroscopy. PIA spectroscopy was performed at a visible-pump, IR-probe setup based on the Spectra-Physics Hurricane system (~120 fs, 800 nm, 1 kHz repetition rate) and two optical parametrical amplifiers (Light Conversion TOPAS) operating in the visible (400–800 nm) and IR (1.2–2.5 μ m) regions (for more details, refer to the Supporting Information). The wavelengths of the excitation pulses were chosen near blend absorption maxima (at 560 and 630 nm for PCDTBT and **P2**, respectively). The wavelength of the probe pulse was set near the maximum of the high-frequency polaron peak at 1.2 μ m (see Figure S8, Supporting Information). The PIA transients were recorded with parallel or perpendicular polarizations with respect to the excitation, from which the isotropic (population) PIA signals were calculated. Films of blends of **P2** and PCDTBT (Sigma-Aldrich) polymers with [70]PCBM (Solenne BV) were spin-coated (1000 rpm, 2 min) from respective solutions on microscope cover-glass substrates.

RESULTS AND DISCUSSION

Synthesis and Investigation of PCDTBTBT (P1). Considering the concept discussed above and outlined in Figure 2, a novel polymer PCDTBTBT (**P1**) can be considered as a promising target. The synthesis of TBTBT building block was performed following the previously reported procedures applied for preparation of similar compounds.²³ Suzuki-type cross-coupling between the 2-thiopheneboronic acid and 4,7-dibromo-2,1,3-benzothiadiazole produced **1** with a reasonable yield (Scheme 1).

Stille cross-coupling between **1** and 2,5-bis(tributylstannyl)-thiophene afforded the target product **2**. Dibromination of

Scheme 1. Synthesis of **P1**



TBTBT in 1,2-dichlorobenzene led to the key monomer **3**. Suzuki–Miyaura polycondensation of **3** with carbazole-based boronic component **4** produced the title polymer **P1**. The optoelectronic characteristics of **P1** are summarized in Table 1.

Table 1. Optoelectronic Properties of Polymers P1, P2, and PCDTBT

polymer	$\lambda_{\text{max}}(\text{sol})$, nm	HOMO, ^a eV	LUMO, eV	$E_g(\text{opt})$, eV
P1	584	-5.53	-3.83	1.70
P2	610	-5.44	-3.79	1.65
PCDTBT	553	-5.50	-3.60	1.90

^aHOMO energies were estimated from onsets of the oxidation potentials using Fermi energy of -5.1 eV for the Fc^+/Fc redox couple.

The absorption spectrum and cyclic voltammogram of **P1** are shown in Figure 3. It is seen from these data that **P1** has

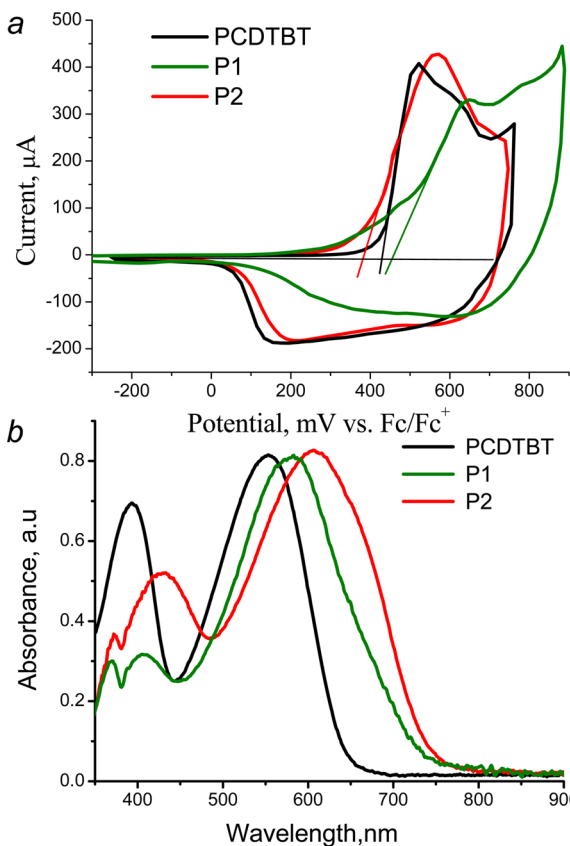


Figure 3. Cyclic voltammograms (a) and absorption spectra (b) of thin films of **P1**, **P2**, and PCDTBT.

significantly lower LUMO energy and narrower band gap compared to PCDTBT. This finding confirmed our initial hypothesis that replacement of TBT unit with extended TBTBT block should improve optoelectronic properties of the polymer.

Indeed, the solar cells based on the **P1**/PCBM blends could potentially deliver higher open circuit voltages (due to lower HOMO energy of **P1**), higher current densities (because of the narrower band gap of **P1**), and higher power conversion efficiencies compared to the PCDTBT/PCBM system. Unfortunately, polymer **P1** showed very low solubility in organic solvents due to the presence of a large planar TBTBT unit in its molecular framework. Therefore, low solubility of **P1**

did not allow us to obtain thin films of reasonable quality required for fabrication of organic solar cells.

Synthesis and Optoelectronic Properties of PCDTTBTBTT (P2**).** In order to overcome the problem of solubility, we have synthesized the conjugated polymer **P2** bearing additional thiophene rings with solubilizing 2-ethylhexyl substituents (Scheme 2). The key monomer **5** can be synthesized from **3** using Suzuki or Stille cross-coupling reactions with corresponding 3-alkylthiophene-based boronic ester (acid) or stannane followed by dibromination of the product using NBS.

The target polymer **P2** obtained in high molecular weights ($M_w = 201\,000$, $M_n = 49\,700$ g/mol, Figure S2) demonstrated reasonably good solubility in organic solvents, which allowed us to perform detailed investigation of optoelectronic and photovoltaic properties of this material. Figure 3 shows that **P2** has significantly reduced band gap compared to PCDTBT. At the same time, both polymers demonstrate very similar oxidation potentials which imply that they have similar HOMO energies (Table 1).²⁴ Consequently, the narrow band gap of 1.65 eV originates mainly from the lower LUMO energy of **P2** as compared to PCDTBT (Figure 1b). Thus, the proposed chemical design based on the use of TBTBT building block provided the material with desired electronic properties as it follows from the energy diagrams for PCDTBT/PCBM and **P2**/PCBM systems shown in Figure 1.

Comparing the properties of **P1** and **P2**, one can also notice that introduction of two additional alkylthiophene rings increases the LUMO and HOMO energies of the polymer and reduces its band gap by 0.05 eV. These changes are expectable since bithiophene units in **P2** induce stronger electron donation effect on the neighboring benzothiadiazole moieties as compared to the thiophenes in **P1**.

The polymer **P2** also demonstrated reasonably good charge transport properties. The SCLC mobility determined for **P2** in hole-only devices was $\sim 2.8 \times 10^{-4} \text{ cm}^2 \text{ V}^{-1} \text{ s}^{-1}$, which is comparable to the mobility estimated for PCDTBT ($\sim 1.2 \times 10^{-4} \text{ cm}^2 \text{ V}^{-1} \text{ s}^{-1}$) and is somewhat lower than the mobility determined for crystalline films of regioregular P3HT ($5.9 \times 10^{-4} \text{ cm}^2 \text{ V}^{-1} \text{ s}^{-1}$, see Figure S3, Supporting Information).

Photovoltaic Properties of **P2.** Photovoltaic properties of **P2** were investigated in conventional bulk heterojunction solar cells which had the following architecture: glass/ITO/PEDOT:PSS/**P2**-PCBM blend/Ca/Ag. The **P2**/PCBM blends were processed from pure 1,2-dichlorobenzene (DCB) and from binary solvents based on DCB–1,8-diiodooctane (DIO) mixtures. Volume concentration of DIO was varied from 0.12 to 6.0%, **P2**:PCBM ratios from 1:1 to 1:4, film thickness from 40 to 200 nm, and different annealing regimes were applied. Such optimization revealed optimal **P2**:PCBM blend composition (1:2 w/w), DIO concentration (0.63%), film thickness (70–80 nm), annealing temperature (90 °C), and time (10 min). The obtained results are given in Table 2.

The organic solar cells based on the **P2**/[70]PCBM blends yielded highly reproducible efficiencies of 5.9–6.1% with the power conversion efficiency of the best device as high as 6.4% (Figure 4 and Figure S4 in Supporting Information).

The revealed optical and electronic properties of the **P2**/[70]PCBM system strongly suggest that it has much higher theoretical potential than the reference PCDTBT/[70]PCBM blends. According to the model introduced by Scharber et al.,¹⁵ it should be possible to reach 9–10% in optimized solar cells based on **P2**/[70]PCBM composites (Figure 5). It is very likely

Scheme 2. Synthesis of P2

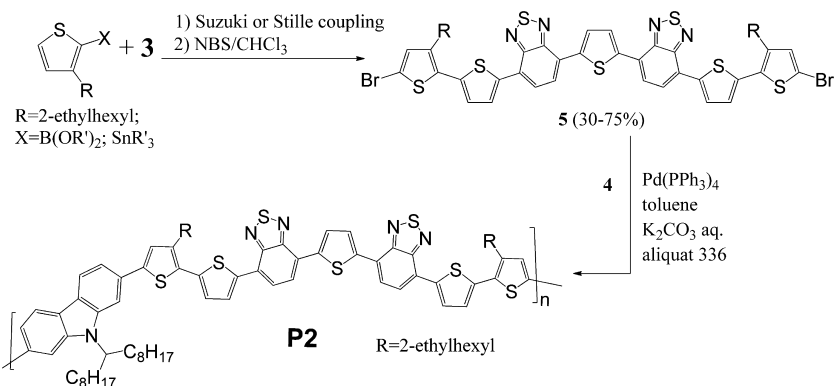


Table 2. Photovoltaic Properties of P2 and PCDTBT Blended with PCBM^a

system	additive	J_{SC} , mA/cm ²	V_{OC} , mV	FF, %	η , %
P2/[70]PCBM (1:2)	no	13.3	730	54	5.3
P2/[70]PCBM (1:2)	0.63% DIO	13.3 (13.6 ^b)	757 (775)	58 (62)	6.0 (6.4)
PCDTBT/[70]PCBM (1:3)	no	12.1	815	60	5.9

^aThe presented values are statistically reproducible results obtained from at least 25 devices. ^bParameters of the best device are given in parentheses.

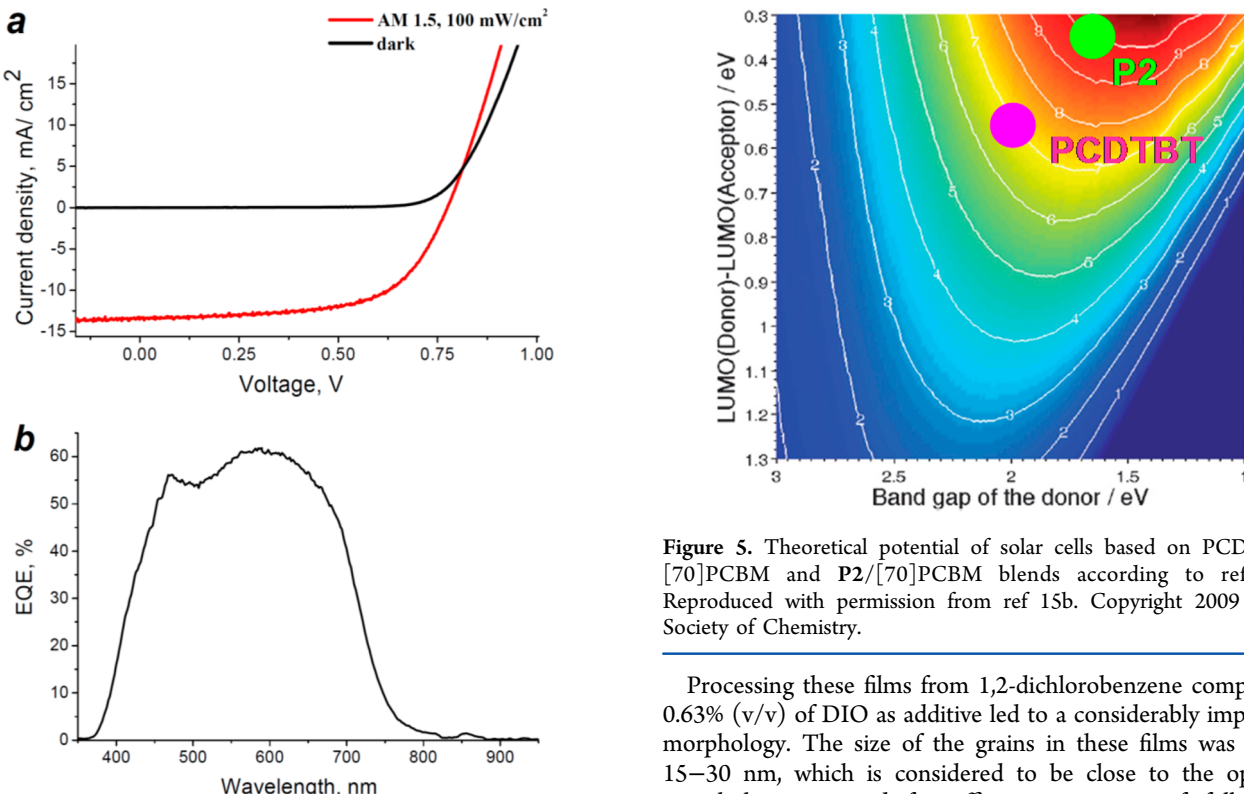


Figure 4. $J-V$ (a) and IPCE (b) characteristics of the best solar cells based on P2/[70]PCBM blend.

that further improvement in the solar cell efficiency can be achieved via thorough optimization of the material itself (polymer **P2**), composite morphology, and the device architecture similarly to the case of PCDTBT.^{15,18}

Atomic Force Microscopy for Composites of P2 with [70]PCBM. The AFM images (Figure 6) of the P2/[70]PCBM composite films cast from pure 1,2-dichlorobenzene revealed poorly organized (almost featureless) structure (Figure 6).

Figure 5. Theoretical potential of solar cells based on PCDTBT/[70]PCBM and P2/[70]PCBM blends according to ref 15b. Reproduced with permission from ref 15b. Copyright 2009 Royal Society of Chemistry.

Processing these films from 1,2-dichlorobenzene comprising 0.63% (v/v) of DIO as additive led to a considerably improved morphology. The size of the grains in these films was about 15–30 nm, which is considered to be close to the optimal morphology required for efficient operation of fullerene/polymer solar cells. The observed evolution of the film surface structure induced by DIO additive correlates also with the improvement in the solar cell performance (Table 2).

It is also notable that thermal annealing of the P2/[70]PCBM composites led to decrease in the film roughness and average grain size. This observation suggests good compatibility between [70]PCBM and polymer P2, which seem to undergo better intermixing at elevated temperatures.

Ultrafast Photoinduced Spectroscopy for P2/[70]PCBM Blends. To evaluate loss channels of initial charge generation, early time exciton and charge dynamics were studied by ultrafast visible-pump–IR-probe photoinduced

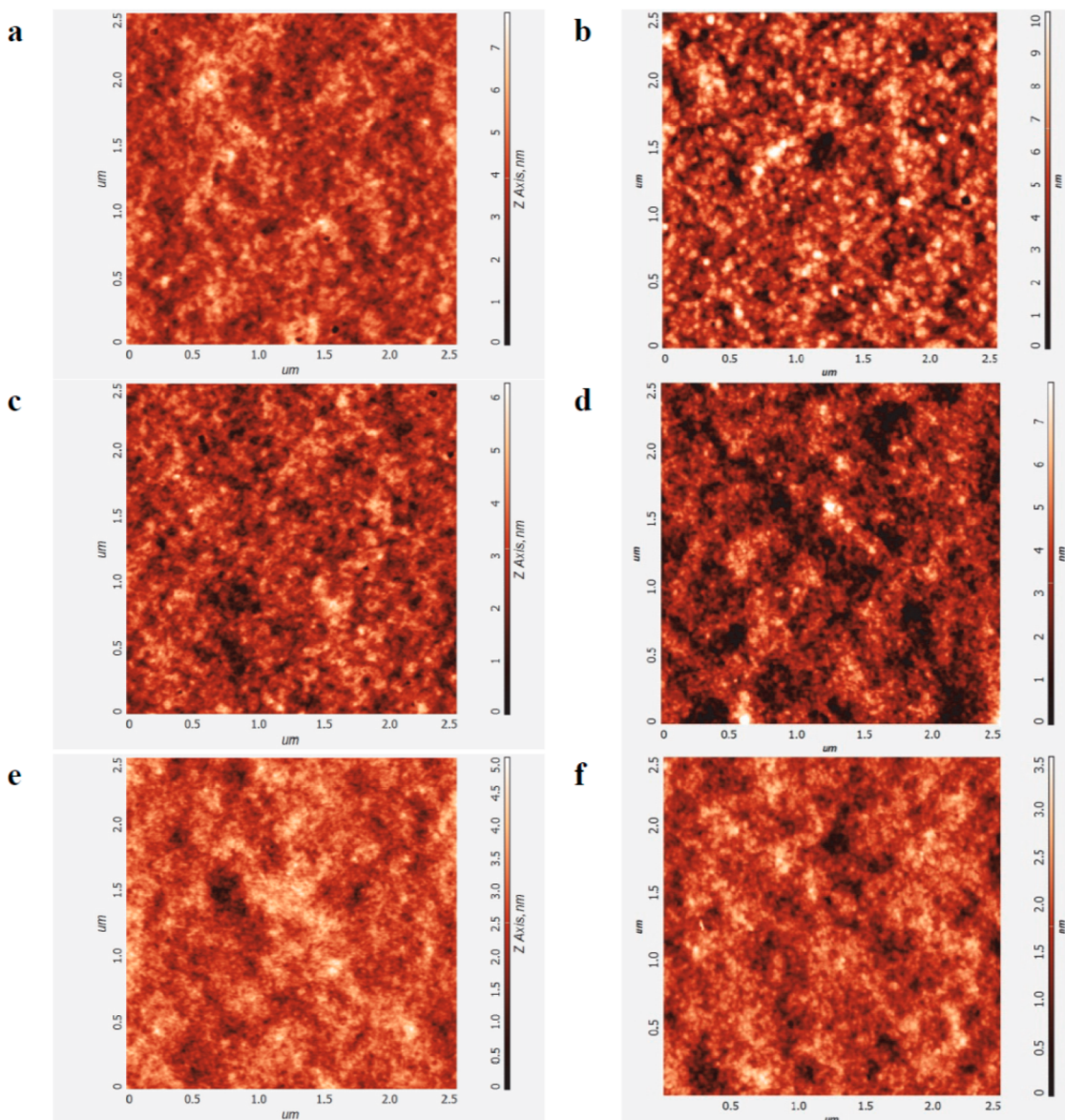


Figure 6. AFM height images for the P2/[70]PCBM blends processed without (a, c, e) and with 0.63% of DIO additive (b, d, f). As-cast films (a, b) were annealed at 90 °C for 10 min (c, d) and then additionally heated at 150 °C for 5 min (e, f).

absorption (PIA) spectroscopy.²⁵ Briefly, the blends were excited by the visible pump pulse close to the absorption maxima (560 and 630 nm for PCDTBT and P2, respectively), and IR (1200 nm) probe pulse was used to monitor the dynamics of photogenerated species (for details, see Supporting Information). Figure 7 shows transient PIA signals for the blends based on P2 and PCDTBT as a reference, with [70]PCBM.

Since polaron and exciton absorption spectra overlap at the probe wavelength (Figure S8, Supporting Information), the PIA dynamics consist of both polaronic and excitonic responses. However, the two responses are readily separated by their time signatures. A fast buildup of the signal near the zero pump–probe delay is due to ultrafast (~100 fs) photogeneration of excitons in the polymer phase. Short-time decay at ~0.2 ps scale is assigned to absorption of polymer excitons and their subsequent dissociation onto separated charges due to electron transfer to [70]PCBM.²⁶ The contribution of the transient exciton absorption decreases

with the increase of [70]PCBM concentration because of decreased share of photons absorbed by the polymer (Figure S12, Supporting Information). All these prove that the reduced to ~0.35 eV LUMO–LUMO offset (Figure 1) does not present any obstacle for efficient dissociation of the polymer excitons.

At longer time scales, the PIA signals increase with characteristic times of tens of picoseconds. This contribution increases with the increase of [70]PCBM concentration. Therefore, these dynamics are assigned to dissociation of [70]PCBM excitons delayed by exciton diffusion in [70]PCBM domains, via the hole transfer process.²⁷ This assignment was verified by substituting [70]PCBM with [60]PCBM which lower absorption led to a substantially diminished amplitude of the signal growth (Figure S10 in Supporting Information).

Hence, at short delays (~1–5 ps) the PIA signals are governed by the charges produced at polymer/[70]PCBM interfaces. They mainly originate from the polymer excitons but also with a small contribution from the [70]PCBM excitons

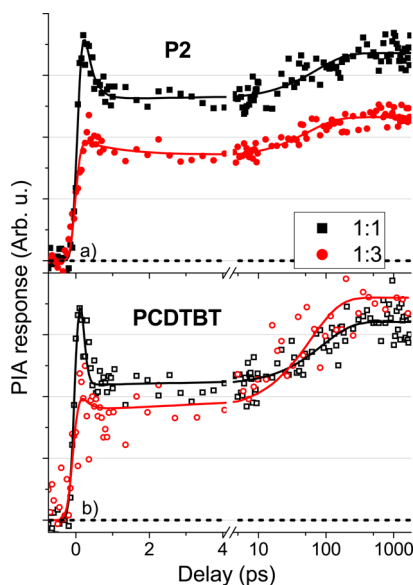


Figure 7. Representative PIA transients for **P2**/[70]PCBM (a) and PCDTBT/[70]PCBM (b) BHJ blends. Symbols show the experimental data points while the solid lines show best fits (see Supporting Information). All transients are normalized by the number of absorbed photons. For the transients with other [70]PCBM concentrations, refer to Figure S9 of the Supporting Information.

that appear to be generated next to the interface. At long delays (>10 ps) the charges are generated from the diffusion-delayed [70]PCBM excitons. Importantly, not all of these excitons will be able to reach the interface due to their finite lifetime of ~ 600 ps.²⁸ Whether the [70]PCBM exciton dies inside the [70]PCBM domain or is harvested at the interface depends on the [70]PCBM domain size, i.e., the bulk heterojunction morphology.

For both polymers, the PIA signal at shot times (for instance, 2 ps) decreases with increasing of [70]PCBM content due to decreased share of polymer absorption (Figure S12, Supporting Information). However, for the PCDTBT-based blends, this decrease is compensated at longer times by efficient harvesting of the [70]PCBM excitons which share in the total blend absorption increases. This indicates close-to-optimal phase separation of the polymer and [70]PCBM constituencies, with [70]PCBM domain sizes less than the exciton diffusion length of ~ 10 nm.²⁹ In contrast, for the **P2**-based blends the amount of separated charges for the 1:3 blend is lower as compared to the 1:1 blend for all delays. This points at the existence of large-sized [70]PCBM clusters from which the [70]PCBM excitons cannot dissociate, thereby suggesting possibilities for further morphology optimization. This corroborates the results obtained from AFM measurements (Figure 6).

Operational Stability of P2 in Devices. It was mentioned above that photostability of conjugated polymers and long-term operation stability of solar cells based on their blends with fullerene derivatives are primary important issues which have to be considered in the design of novel materials for organic photovoltaics. We investigated photostability of thin polymer films under continuous illumination with the light coming from luminescent lamps inside argon glovebox (light power ~ 60 mW/cm²; temperature of 75–85 °C; O₂ and H₂O concentrations below 1 ppm). Polymers **P2** and PCDTBT did not show any noticeable photobleaching within 6000 h. This result agrees well with the previous reports on photostability of

PCDTBT.¹⁴ On the contrary, such reference polymers as P3HT, PTB7, and MDMO-PPV underwent substantial degradation under the specified conditions (change in the optical density of the films by more than 10% was observed).

The operation stability of organic solar cells was investigated under very similar conditions (metal halide lamps, temperature 80–85 °C). The device architecture was ITO/PEDOT:PSS-(Clevios PH)/[60]PCBM-polymer blend/Mg/Al. It is seen from Figure 8 that solar cells based on **P2** and PCDTBT

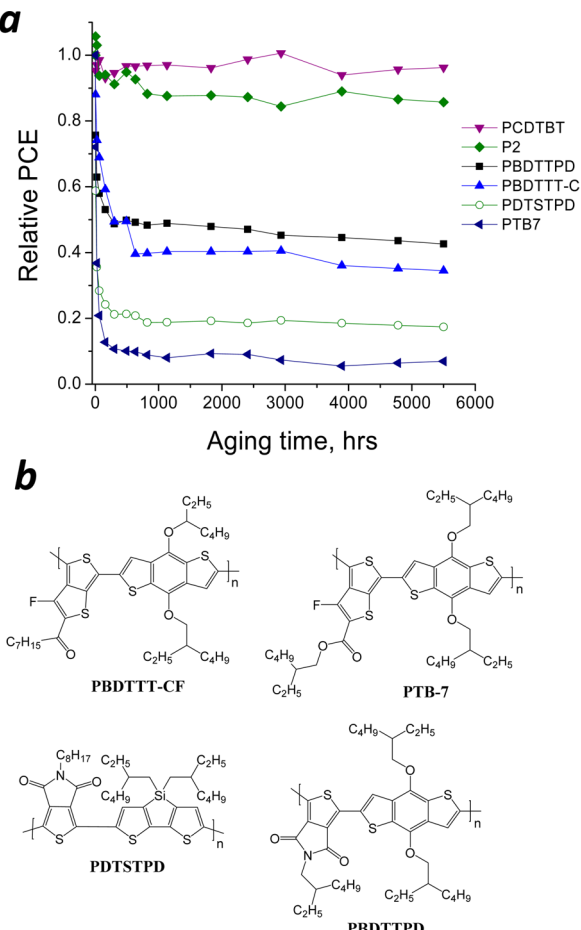


Figure 8. Operation stability of organic solar cells based on the blends of different polymers with [60]PCBM (a) and molecular structures of the reference polymers used in the study (b).

demonstrate much superior stability compared to the similar devices comprising reference polymer materials such as PTB7, PBDDTT-CF, and PDTSTPD.

The analysis and discussion of the degradation processes occurring in these devices lie outside the scope of the present work and will be reported elsewhere. The obtained results strongly suggest that combinations of carbazole, thiophene, and benzothiadiazole units in **P2** and PCDTBT are responsible for advanced stability of these materials. From this perspective, polymer **P2** reported herein is considered as a promising platform for construction of organic solar cells with improved long-term stability, particularly in inverted device architectures.

CONCLUSION

In conclusion, we have shown that alternating copolymers of novel (-X-DADAD)_n family demonstrate superior optical and electronic properties compared to the conventional (-X-DAD)_n

analogues such as PCDTBT. The first designed copolymer of this family (**P2**) comprising TBTBT as a key building block routinely demonstrated power conversion efficiencies exceeding 6% in bulk heterojunction solar cells with a potential for improvement up to 9–10%. The developed in this work approach might be successfully transferred to other conjugated polymers comprising DAD units in their molecular frameworks. We believe that practical realization of this concept represents a promising pathway toward designing novel donor polymers for highly efficient and stable organic solar cells.

ASSOCIATED CONTENT

Supporting Information

GPC profile and NMR spectra for **P2**; SCLC data for P3HT, PCDTBT, and **P2**; detailed description of ultrafast PIA spectroscopy. This material is available free of charge via the Internet at <http://pubs.acs.org>.

AUTHOR INFORMATION

Corresponding Author

*E-mail troshin2003@inbox.ru; Tel +7-496-522-1418 (P.A.T.).

Notes

The authors declare no competing financial interest.

ACKNOWLEDGMENTS

We thank Mrs. E. Levchenkova and Mrs. Z. Dzhivanova for participation in the solar cell stability studies. Dr. D. V. Novikov is acknowledged for support with the electrochemical measurements. The major part of this work was funded by Lanxess Germany. Investigation of some properties of **P1** and **P2** was also supported by Russian President Science Foundation (MK-5260.2014.3) and Russian Foundation for Basic Research (14-03-31681-mol-a). O.V.K. acknowledges “Aurora - Towards Modern and Innovative Higher Education” programme and Russian Foundation for Basic Research, research project No. 14-02-31632, for financial support.

REFERENCES

- (1) (a) Service, R. F. *Science* **2011**, *332*, 293. (b) Ameri, T.; Li, N.; Brabec, C. J. *Energy Environ. Sci.* **2013**, *6*, 2390. (c) Duan, C.; Zhang, K.; Zhong, C.; Huang, F.; Cao, Y. *Chem. Soc. Rev.* **2013**, *42*, 9071.
- (2) Wang, E.; Hou, L.; Wang, Z.; Hellström, S.; Zhang, F.; Inganäs, O.; Andersson, M. R. *Adv. Mater.* **2010**, *22*, 5240.
- (3) Mühlbacher, D.; Scharber, M.; Morana, M.; Zhu, Z.; Waller, D.; Gaudiana, R.; Brabec, C. *Adv. Mater.* **2006**, *18*, 2884.
- (4) Wienk, M. M.; Turbiez, M.; Gilot, J.; Janssen, R. A. J. *Adv. Mater.* **2008**, *20*, 2556.
- (5) Liang, Y.; Wu, Y.; Feng, D.; Tsai, S.-T.; Son, H.-J.; Li, G.; Yu, L. J. *Am. Chem. Soc.* **2009**, *131*, 56.
- (6) (a) Piliego, C.; Holcombe, T. W.; Douglas, J. D.; Woo, C. H.; Beaujuge, P. M.; Frechet, J. M. J. *J. Am. Chem. Soc.* **2010**, *132*, 7595. (b) Chu, T.-Y.; Lu, J.; Beaupre, S.; Zhang, Y.; Pouliot, J.-R.; Wakim, S.; Zhou, J.; Leclerc, M.; Li, Z.; Ding, J.; Tao, Y. *J. Am. Chem. Soc.* **2011**, *133*, 4250.
- (7) Wang, E.; Ma, Z.; Zhang, Z.; Vandewal, K.; Henriksson, P.; Inganäs, O.; Zhang, F.; Andersson, M. R. *J. Am. Chem. Soc.* **2011**, *133*, 14244.
- (8) Moulé, A. J.; Tsami, A.; Bünnagel, T. W.; Forster, M.; Kronenberg, N. M.; Scharber, M.; Koppe, M.; Morana, M.; Brabec, C. J.; Meerholz, K.; Scherf, U. *Chem. Mater.* **2008**, *20*, 4045.
- (9) Liang, Y.; Xu, Z.; Xia, J.; Tsai, S.-T.; Wu, Y.; Li, G.; Ray, C.; Yu, L. *Adv. Mater.* **2010**, *22*, E135.
- (10) Hou, J.; Chen, H.-Y.; Zhang, S.; Li, G.; Yang, Y. *J. Am. Chem. Soc.* **2008**, *130*, 16144.
- (11) (a) Cheng, Y.-J.; Yang, S.-H.; Hsu, C.-S. *Chem. Rev.* **2009**, *109*, 5868. (b) Chen, J.; Cao, Y. *Acc. Chem. Res.* **2009**, *42*, 1709. (c) Gendron, D.; Leclerc, M. *Energy Environ. Sci.* **2011**, *4*, 1225. (d) Szarko, J. M.; Guo, J.; Rolczynski, B. S.; Chen, L. X. *J. Mater. Chem.* **2011**, *21*, 7849. (e) Son, H. J.; Carsten, B.; Jung, I. H.; Yu, L. *Energy Environ. Sci.* **2012**, *5*, 8158. (f) Yeh, N.; Yeh, P. *Renewable Sustainable Energy Rev.* **2013**, *21*, 421. (g) Zhou, H.; Yang, L.; You, W. *Macromolecules* **2012**, *45*, 607.
- (12) (a) Jørgensen, M.; Norrman, K.; Gevorgyan, S. A.; Tromholt, T.; Andreasen, B.; Krebs, F. C. *Adv. Mater.* **2012**, *24*, 580. (b) Po, R.; Bernardi, A.; Calabrese, A.; Carbonera, C.; Corso, G.; Pellegrino, A. *Energy Environ. Sci.* **2014**, *7*, 925. (c) Uk J. Lee; Jung, J. W.; Jo, J. W.; Jo, W. H. *J. Mater. Chem.* **2012**, *22*, 24265.
- (13) Blouin, N.; Michaud, A.; Leclerc, M. *Adv. Mater.* **2007**, *19*, 2295.
- (14) Peters, C. H.; Quintana, I. T. S.; Kastrop, J. P.; Beaupré, S.; Leclerc, M.; McGehee, M. D. *Adv. Energy Mater.* **2011**, *1*, 491.
- (15) (a) Scharber, M. C.; Mühlbacher, D.; Koppe, M.; Denk, P.; Waldauf, C.; Heeger, A. J.; Brabec, C. J. *Adv. Mater.* **2006**, *18*, 789. (b) Ameri, T.; Dennler, G.; Lungenschmied, C.; Brabec, C. J. *Energy Environ. Sci.* **2009**, *2*, 347–363.
- (16) (a) Park, S. H.; Roy, A.; Beaupré, S.; Cho, S.; Coates, N.; Moon, J. S.; Moses, D.; Leclerc, M.; Lee, K.; Heeger, A. J. *Nat. Photonics* **2009**, *3*, 297. (b) Seo, J. H.; Gutacker, A.; Sun, Y.; Wu, H.; Huang, F.; Cao, Y.; Scherf, U.; Heeger, A. J.; Bazan, G. C. *J. Am. Chem. Soc.* **2011**, *133*, 8416–8419. (c) Fang, G. J.; Liu, Y.; Fu, B.; Meng, B.; Zhang, Z.; Xie; Wang, L. *Org. Electron.* **2012**, *13*, 2733–2740. (d) He, Z.; Zhong, C.; Huang, X.; Wong, W.-Y.; Wu, H.; Chen, L.; Su, S.; Cao, Y. *Adv. Mater.* **2011**, *23*, 4636–4643.
- (17) Banerji, N.; Gagnon, E.; Morgantini, P.-Y.; Valouch, S.; A. Mohebbi, R.; Seo, J.-H.; Leclerc, M.; Heeger, A. J. *J. Phys. Chem. C* **2012**, *116*, 11456.
- (18) (a) Love, J. A.; Collins, S. D.; Nagao, I.; Mukherjee, S.; Ade, H.; Bazan, G. C.; Nguyen, T.-Q. *Adv. Mater.* **2014**, *26*, 7308. (b) Liu, X.; Hsu, B. B. Y.; Sun, Y.; Mai, C.-K.; Heeger, A. J.; Bazan, G. C. *J. Am. Chem. Soc.* **2014**, *136*, 16144. (c) Lai, L. F.; Love, J. A.; Sharenko, A.; Coughlin, J. E.; Gupta, V.; Tretiak, S.; Nguyen, T.-Q.; Wong, W.-Y.; Bazan, G. C. *J. Am. Chem. Soc.* **2014**, *136*, 5591. (d) Liu, X.; Sun, Y.; Hsu, B. B. Y.; Lorbach, A.; Qi, L.; Heeger, A. J.; Bazan, G. C. *J. Am. Chem. Soc.* **2014**, *136*, 5697. (e) Love, J. A.; Nagao, I.; Huang, Y.; Kuik, M.; Gupta, V.; Takacs, C. J.; Coughlin, J. E.; Qi, L.; van der Poll, T. S.; Kramer, E. J.; Heeger, A. J.; Nguyen, T.-Q.; Bazan, G. C. *J. Am. Chem. Soc.* **2014**, *136*, 3597. (f) Chen, X.; Liu, X.; Burgers, M. A.; Huang, Y.; Bazan, G. C. *Angew. Chem., Int. Ed.* **2014**, *53*, 14378. (g) Ko Kyaw, A. K.; Gehrig, D.; Zhang, J.; Huang, Y.; Bazan, G. C.; Laquai, F.; Nguyen, T.-Q. *J. Mater. Chem. A* **2015**, *3*, 1530. (h) Coughlin, J. E.; Henson, Z. B.; Welch, G. C.; Bazan, G. C. *Acc. Chem. Res.* **2014**, *47*, 257.
- (19) Wienk, M. M.; Kroon, J. M.; Verhees, W. J. H.; Knol, J.; Hummelen, J. C.; van Hall, P. A.; Janssen, R. A. J. *Angew. Chem., Int. Ed.* **2003**, *42*, 3371.
- (20) Chang, D. W.; Ko, S.-J.; Kim, G.-H.; Bae, S.-Y.; Kim, J. Y.; Dai, L.; Baek, J.-B. *J. Polym. Sci., Part A: Polym. Chem.* **2012**, *50*, 271–279.
- (21) Akkuratov, A. V.; Susarova, D. K.; Moskvin, Y. L.; Anokhin, D. V.; Chernyak, A. V.; Prudnov, F. A.; Novikov, D. V.; Babenko, S. D.; Troshin, P. A. *J. Mater. Chem. C* **2015**, *3*, 1497.
- (22) Troshin, P. A.; Hoppe, H.; Renz, J.; Egginger, M.; Mayorova, J. Y.; Goryachev, A. E.; Peregudov, A. S.; Lyubovskaya, R. N.; Gobsch, G.; Sariciftci, N. S.; Razumov, V. F. *Adv. Funct. Mater.* **2009**, *19*, 779.
- (23) (a) Melucci, M.; Favaretto, L.; Zanelli, A.; Cavallini, M.; Bongini, A.; Maccagnani, P.; Ostoja, P.; Derue, G.; Lazzaroni, R.; Barbarella, G. *Adv. Funct. Mater.* **2010**, *20*, 445. (b) Moriwaki, S.; Goto, O.; Asada K. Sumitomo Chemical Company, Ltd., European patent application EP2327734 A, 2009.
- (24) Cardona, C. M.; Li, W.; Kaifer, A. E.; Stockdale, D.; Bazan, G. C. *Adv. Mater.* **2011**, *23*, 2367.
- (25) Bakulin, A. A.; Martyanov, D. S.; Paraschuk, D. Y.; Pshenichnikov, M. S.; van Loosdrecht, P. H. M. *J. Phys. Chem. B* **2008**, *112* (44), 13730–13737.
- (26) (a) Grancini, G.; Martino, N.; Antognazza, M. R.; Celebrano, M.; Egelhaaf, H.-J.; Lanzani, G. *J. Phys. Chem. C* **2012**, *116* (17),

- 9838–9844. (b) Guo, J.; Ohkita, H.; Benten, H.; Ito, S. *J. Am. Chem. Soc.* **2010**, *132* (17), 6154–6164.
- (27) Bakulin, A. A.; Hummelen, J. C.; Pshenichnikov, M. S.; van Loosdrecht, P. H. M. *Adv. Funct. Mater.* **2010**, *20* (10), 1653–1660.
- (28) Hedley, G. J.; Ward, A. J.; Alekseev, A.; Howells, C. T.; Martins, E. R.; Serrano, L. A.; Cooke, G.; Ruseckas, A.; Samuel, I. D. W. *Nat. Commun.* **2013**, *4*, 2867.
- (29) (a) Koeppe, R.; Sariciftci, N. S. *Photochem. Photobiol. Sci.* **2006**, *5* (12), 1122–1131. (b) Cook, S.; Furube, A.; Katoh, R.; Han, L. *Chem. Phys. Lett.* **2009**, *478* (1–3), 33–36.